Seascape Modeling lab
University of Maine School of Marine Sciences
www.seascapemodeling.org

Shore-based Photogrammetry of Surface Oceanography for Oil Spill Mitigation

Seascape Modeling Lab Report 2010.A

Nicholas R. Record*, Jonathan D. Whitefield, Andrew J. Pershing,
Giles Kingsley, Kathi Higgins

* *Corresponding author*
350 Commercial St. Portland ME 04101
(207)-228-1670
nrecord@gmri.org

Abstract

We deployed cameras for sea surface photogrammetry in Portland Harbor, Maine to collect data for a one year pilot study. One camera was installed in the control booth in the Casco Bay Bridge between Portland and South Portland, and the other was installed in the Gulf of Maine Research Institute. The cameras collected one image per minute during daylight hours from June 2008 to May 2009. We deployed a meteorological station during the same period to collect wind speed and direction data. Here we present a description of the system, the raw data, tidal data from Portland Harbor, and some preliminary analysis.

Acknowledgements

We would like to thank the personnel in the control booth on the Casco Bay Bridge—in particular, Warren Knowles, Bill Johnson, and Bonnie LaPointe—for allowing us to use their space, and for their friendliness and helpfulness during this project. Funding was provided by the Maine Sea Grant Program and the Maine Oil Spill Advisory Committee.

Table of Contents

List of Figures

List of Tables

Introduction

Portland is the third largest oil terminal port in the United States, and together with the ports of Searsport and Eastport, Maine ports receive a major portion of the oil arriving in New England. To enter these ports, tankers must traverse some of the most lucrative fishing grounds in the world and pass by fragile wetland and salt marsh habitats. The potential impacts of an oil spill in Maine were made abundantly clear during the 1996 spill of the *Julie N* in Portland Harbor (Maine DEP, 1998). After colliding with a bridge, the *Julie N* began to leak fuel oil. She was quickly brought alongside the commercial pier and surrounded by booms. Quick securing of the vessel combined with intensive mitigation resulted in containment of 98% of the oil; however, that meant an estimated 179,634 gallons entered Portland Harbor and Casco Bay, closing fishing and lobstering for 2.5 months, interfering with commercial traffic into the port, and contaminating 25.6 acres of wetlands.

As demonstrated by the *Julie N* spill, clean up and mitigation of an oil spill in the marine environment requires a combination of pre-planning and flexible reaction. For example, in the event of a spill in Casco Bay, the Marine Spill Response Corporation would respond by placing booms at strategic locations determined months or years previously. The locations of the booms would be selected to minimize the impact on fragile habitats, such as the Presumpscot River wetlands, and to aid in collection and clean up. These locations are based on estimates of the mean surface circulation from both observations and models. Clean up crews would also track the spill and deploy recovery gear depending on the peculiarities of an individual spill. Both planning and response would greatly benefit from information on circulation features that would tend to transport and accumulate oil.

Oil, especially lighter fuel oils, spreads along a thin layer over the water's surface. After the initial spreading, the oil layer will begin to respond to the movements of the water underneath it. Oil will tend to accumulate in convergent features such as Langmuir cells. In the days following the *Julie N* spill, aerial surveys reported oil accumulating in rows—consistent with Langmuir-like features (Maine DEP, 1998). Knowing the locations and trajectories of these surface features would facilitate better planning and allow clean up crews to collect oil more efficiently. Oceanographers have developed detailed numerical models of ocean circulation. These models have been used for pre-sighting of booms and for predicting the movement of spills in open water (Reed, 1999); however, due to their complexity, many important fine-scale processes, such as Langmuir circulation, are not included in the fine scale numerical models that are used to predict dispersion of spilled oil (Thorpe, 2004).

Knowing the locations and trajectories of these surface features would facilitate better planning and allow clean up crews to collect oil more efficiently. Oceanographers have developed detailed numerical models of ocean circulation. These models have been used for pre-sighting of booms and for predicting the movement of spills in open water (Reed, 1999); however, due to their complexity, many important fine-scale processes, such as Langmuir circulation, are not included in the fine scale numerical models that are used to predict dispersion of spilled oil (Thorpe, 2004).

While it is usually impractical to generate oil spills for experiments, naturally occurring visible slicks are common in coastal waters. These slicks are generally biogenic films in the marine surface microlayer, that show area of convergence along which buoyant material collects (Huehnerfuss, 2006). The surface tension gradient caused by the presence of the biogenic layer dampens capillary waves, generating a visual contrast between the convergence zone and the divergence zone, so that slicks are easily observed from the ocean surface (Wu, 1983). This gradient in surface tension may be weaker

with crude oil than with naturally occurring biogenic films, depending on the type of oil spilled and the length of time it has been in the water, but the behavior and appearance of the surface film are very similar (Alpers and Espedal, 2004). In particular, the viscosity of crude oil has a wave dampening effect so similar to that of biogenic films that a great deal of effort has been devoted to the difficult task of distinguishing the two types of slicks in remote sensing (Huehnerfuss et al., 1986; Gade et al., 1998; Alpers and Espedal, 2004).

We developed a low-cost system to take advantage of these natural oil slicks by measuring surface features and monitoring their movement. The system uses low-cost digital cameras and a mapping program to produce georectified animations of surface flows. The system can be used for spill preparation as well as response, and has other potential applications. We tested a range of range of system configurations, from very low cost to relatively high cost, and both operational and data-collection modes.

The specific goals of the project were: (1) to develop this low-cost system, (2) evaluate image processing algorithms for identifying slicks and tracking their movement, (3) identify persistent convergence features and their associations with weather, tide, season, etc., and (4) perform a cost analysis of the different configurations for this system. In this report, we describe (1), and present the data collected during a one-year deployment in Portland Harbor.

System Overview

The system is composed of two parts: the hardware for time-lapse image collection, and the algorithms for rectifying the imagery. The hardware consists of a camera, and a configuration of equipment to trigger the camera and store or transmit the image files. The configuration depends on the site and the requirements of the study. The rectification algorithms are written in the MATLAB programming language.

For the purposes of development, we tested two system configurations, deployed in Portland Harbor. The two systems were deployed at the Gulf of Maine Research Institute (GMRI) and the Casco Bay Bridge, obtaining two simultaneous views of the harbor (figure 1). The first system was a low-cost, low-resolution option, for use within range of a wireless network (figure 2). The second was a high-resolution, stand-alone system, capable of long-term deployment (figure 3). The specifications of these two systems are outlined in table 1. The cost versus performance trade-off between these two systems is detailed in a separate report.

Rectification of Images

The rectification algorithm combines methods from previous work in three steps: (1) lens distortion correction, (2) rectification, and (3) ground controlled error minimization. The lens distortion correction builds on the work of (Holland et al. 1997). The algorithm takes a series of points that should fall on a straight line or comprise a series of lines, and corrects them based on the equation:

$$\Delta r = k_1 r^3 + k_2 r$$

where r is the radial distance from the center of the image. The parameters k_1 and k_2 are chosen to minimize the deviation from linearity of the set of control points The rectification follows Pawlowicz's (2003) procedure, which rectifies oblique ocean surface images using information on the position and angle of the camera. The error minimization follows Bourgault's (2008) technique, which uses ground control points and a regression model to minimize the error in the rectification. Ground control points are collected either with a GPS system, or by identifying points in a georectified aerial photograph.

The algorithm produced accurate maps of sea surface features (figure 4). Resolution varied depending on distance from the camera, ranging from ~ 1m very near to the camera to ~100m near the mouth of the harbor (figure 5). Movement of the camera due to bridge openings, traffic, and wind added a small amount of error to the rectification as well. This error, when pronounced, can be manually rectified.

Outreach Activities

The primary mode of outreach for this project is a series of reports, describing the system, the data, and opportunities for future work. Other outreach activities include the following.

The lab website (http://www.seascapemodeling.org/seascape_projects) provides updates on all of our lab projects. A sub-category of the blog is devoted to this project, documenting progress, and providing discussion. The entries relevant to this project can be found at the following link:

http://www.seascapemodeling.org/seascape_projects/sea-surface-photogrammetry/

In 2009, the site generated over 3,000 hits from over 1,000 unique viewers. Of all web traffic to the site, 88% came from within the United States, and 65% came from within Maine. The site has led to inquiries regarding duplication of our system for use at other locations.

The LabVenture! program at the Gulf of Maine Research Institute brings fifth-grade classes from throughout Maine to participate in a half-day interactive science program. Part of this program is a 15 minute segment entitled Today in the Gulf of Maine (TGoM), where students learn about current active research in the Gulf of Maine. We composed a TGoM module based on this project and presented it to 10 groups, each of roughly 50 students, during 2008.

We are currently working with a group in the Ecology Department at the Centro de Investigación Científica y de Educación Superior de Ensenada (CICESE) to apply the camera system to a red tide monitoring program on the west coast of Mexico.

Review of data

Data presented in this section are from the Nikon D40x camera mounted in the Casco Bay Bridge control booth. The images from the low-cost Panasonic network camera have not yet been analyzed.

The camera started taking images at just before noon Eastern Daylight time (EDT, GMT–4 hours) on May 27, 2008. However, the final position of the camera had not been established, and as a result, the first useable images begin at exactly noon on May 27, 2008. From this point on, the camera captured one picture every minute, with images being taken from just before sunrise until just after sunset. This allowed the maximum number of pictures to be taken per day.

Images were taken between 5:00am EDT and 9:59pm EDT during the range of May 2008 to the end of October 2008. The hours of operation were then shortened to 6:00am Eastern Standard time (EST, GMT–5 hours) until 7:59pm EST for the months of November and December 2008. All data collected in 2009 were taken over the hours of 5am until 8:59pm, with January until 8 March being recorded in EST, and 9 March until mid-May being EDT. These regular images continued for approximately one year, with the final images being taken at 9:54am EDT on May 15, 2009. Over the sample period of 354 days, a total of 307,674 images were recorded (table 2).

There were several occasions in which the camera or computer did not record an image, resulting in 15 days that do not have complete records (excluding the first and last days of the deployment). These occurrences normally resulted in data drop-outs that only lasted for a couple of images. However, there were 4 days where the number of images lost meant that less than half the complete day was available. These instances all occurred at the end of 4 blocks where no data were recorded for the entire day.

Data were lost over a 6 day period from Oct 17-22, 2008, and then another three times in December and January. The camera stopped recording at 6:32pm on December 3 (meaning that most of the day was recorded) and was not restarted again until 5:55pm on December 11. The system then froze again at 4:01pm on December 15, and was restored at 2:03pm on December 17. The final, and longest gap in data occurs between 12:11pm on December 30 and lasted until 1:39pm on January 15, 2009. Figure 6 shows the availability of all data.

Likely causes for the absences include power outages caused by weather (a large ice storm hit New England in December 2008, causing power to be lost for several days), or other unforeseen computer glitches. Acquisition was restarted by manually rebooting the computer, as the hardware was not connected to any form of network or remote control source.

Missing data meant that there were 304 days where a complete day of data was available (i.e. data existed continuously from before sunrise to after sunset). However, weather conditions also impacted the quality of the images. Days were grouped in to three distinct categories: clear, questionable, and poor. These categories were defined as the visibility seen on the noon-time image. Examples of these conditions are shown in figure 7(a) – 7(c).

Clear visibility was an image where the horizon could be seen, and light conditions were good enough to be able to visually identify slick areas in the image. An image with the horizon partially obscured, but the majority of the image clear was labeled “questionable”. This was because by only looking at the noon-time image, it was not possible to determine whether this was the worst that the conditions got during that day. The final category, “poor”, was applied to those images where light levels were insufficient to visually identify slick areas, or when visibility was reduced to the front half of the image or less.

These categories provide a first-level quality check, but cannot be relied upon as a definitive measure. It is intended that a quality check will be performed on all images, as there are certain times that a small number of images are unusable, despite the noon-time image suggesting that the specified day is in fact clear. Examples of these are shown in figure 7(d) – 7(f), and include ships passing under the Casco Bay Bridge, sea birds passing in front of the field of view, and also meteorological occurrences such as sea smoke, as shown in figure 7(f), or passing squalls.

Of the 304 days with a complete record of images, 21 of them would be rejected due to low or zero visibility at noon. An additional 14 days were recorded as "questionable". This meant that 269 days, or 76% of the days can be regarded as "perfect", in that they have both clear visibility and an uninterrupted day of images, and 81.9% of days can be regarded as "good"; these days have complete records and either clear or questionable visibility. If data are included from the partial days (i.e. those that have only some records missing), then the number of "questionable" days increases by one, and the number of clear days changes to 284. This returns a value of 86.2% of days that are useable, or that have clear/questionable visibility and the majority of images available. These values are likely to change slightly, however, if a more robust quality checking system is implemented.

Meteorological data, specifically wind direction and speed, were taken from the weather station located at the Gulf of Maine Research Institute. There were periodic data drop-outs, as the data were transmitted over a wireless connection. Occasionally data would not be stored on the computer through reasons unknown. Weather data exist for 224 days, or 63.3%, of the study period. The range of meteorological data available is shown on figure 8 (wind velocity) and figure 9 (wind direction).

Tidal data were recorded at the NOAA station ID 8418150, marked as a diamond in figure 1. Data were downloaded from the NOAA Center for Operational Oceanographic Products and Services (CO-OPS) website (http://co-ops.nos.noaa.gov/data_menu.shtml?stn=8418150%20Portland,%20ME&type=Tide%20Data) as both a 6 minute average of water level, and as time of high and low tides. These data were available and quality checked as being of usable quality for the entire study period, as seen in figure 10.

	Casco Bay Bridge	**GMRI**
Camera	Nikon D40x	Panasonic network camera
Pixel resolution	3872 × 2592	640 × 480
Photo file size	3.1 MB	48 KB
Computer on site	Mac Mini	none
Data storage at site	320 GB	none
Communication	none	Wireless network

Table 1. Specifications of the camera systems used at each study site.

Date (month/year)	Total images	# clear days	Weather data	Tidal data
May 2008[1]	4,680	5	1	5
June 2008	30,295	27	24	30
July 2008	31,614	30	30	31
August 2008	31,613	26	8	31
September 2008	30,595	26	10	30
October 2008	22,447	22	22	31
November 2008	25,195	22	13	30
December 2008	16,286	17	12	31
January 2009	15,800	15	22	31
February 2009	26,862	27	24	28
March 2009	29,760	26	20	31
April 2009	28,792	28	23	30
May 2009[2]	13,735	14	15	15
TOTAL	307,674	285	224	354

[1] Data acquisition began at 12:00pm EDT on 27 May 2008
[2] Data acquisition ended at 3:09pm EDT on 15 May 2009

Table 2. Monthly metadata. Each month summarizes the total number of images available, as well as the approximate number of days where image quality is good. Also shown are the number of days weather data (wind speed and direction) are available from the GMRI meteorological station and the number of days that data were downloaded from the NOAA tidal gauge.

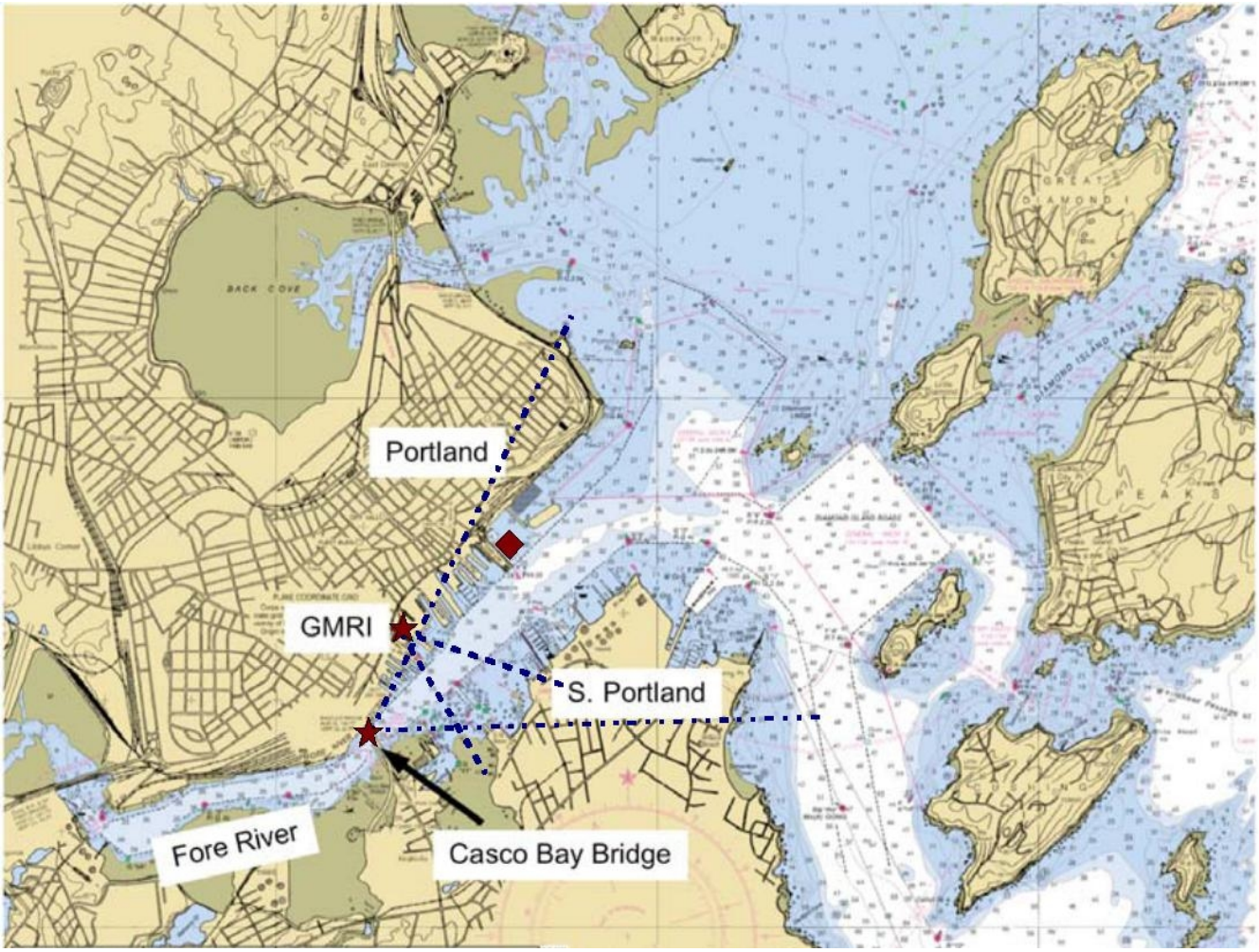

Figure 1. Study site: Portland Harbor, Maine. Stars indicate camera locations. Dashed lines indicate camera fields of view. Diamond indicates the location of the tidal gauge. The meteorological station is located at GMRI.

Figure 2. Camera system installed in the GMRI site.
System included: Panasonic network camera (see table 1).

Figure 3. Camera system installed in Casco Bay Bridge site. System included: Nikon D40x SLR camera, Mac Mini computer, 2 external hard drives (see table 1).

(a)

(b)

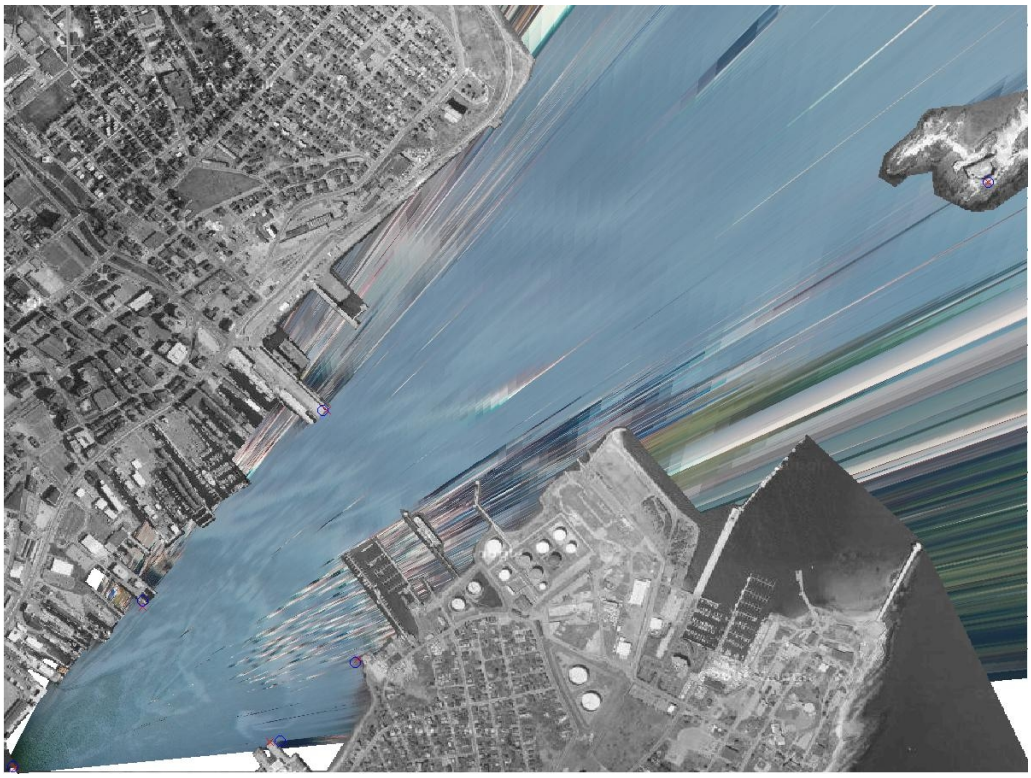

Figure 4. An example of an image **(a)** before, and **(b)** after georectification. Crosses and circles indicate ground control points.

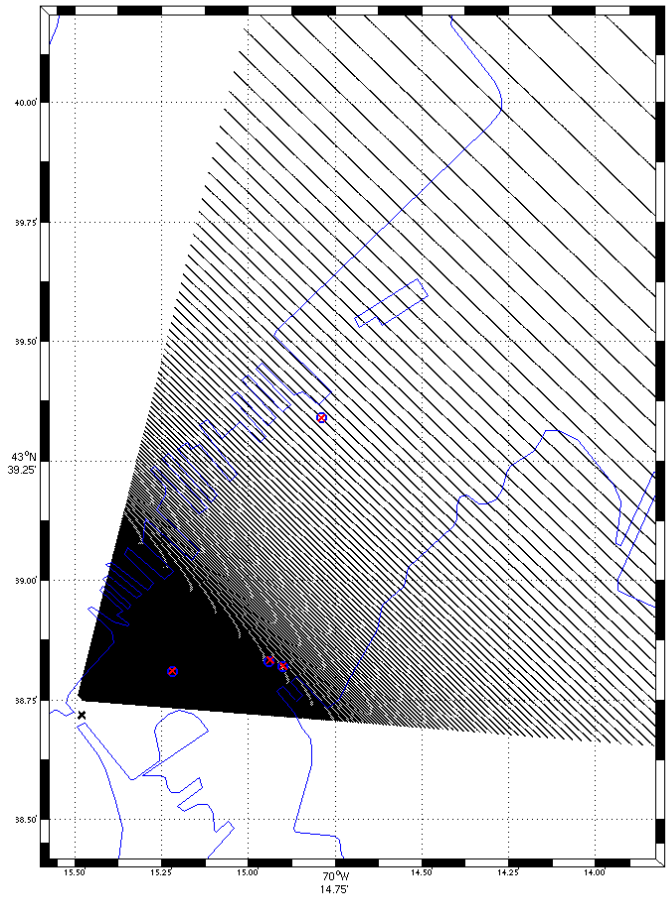

(a)

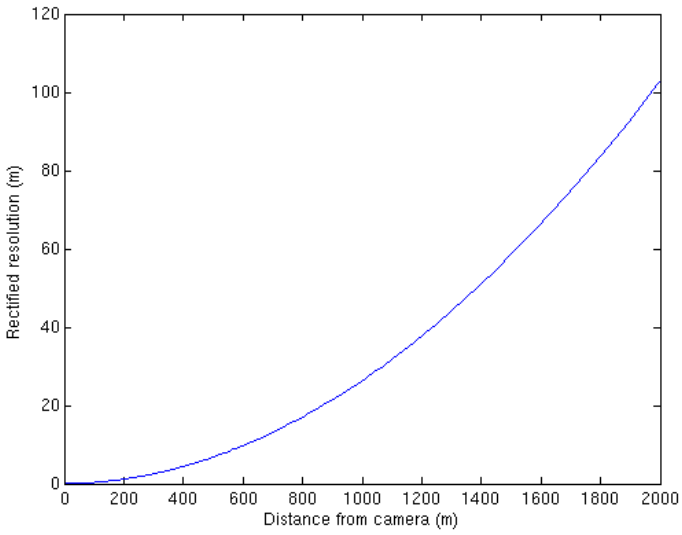

(b)

Figure 5. Image resolution after georectification process. **(a)** shows where the position of each pixel from the original image is mapped to on the rectified image. **(b)** shows the resolution of each pixel with respect to the original distance from the camera.

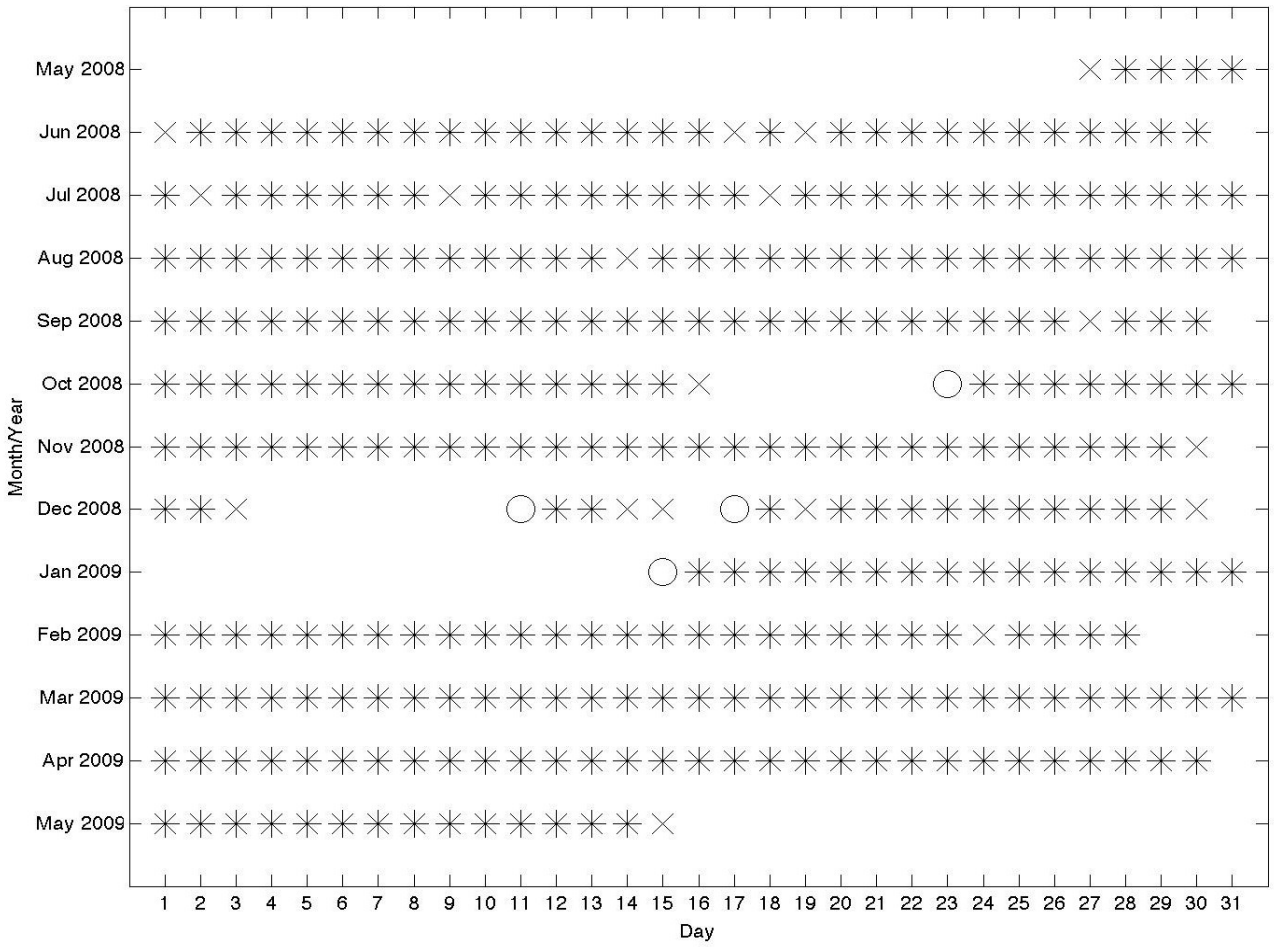

Figure 6. Data availability. (*) signifies a day with uninterrupted data. (X) is a day where there is missing images, but less than half the day is missing. (O) shows days where the majority of data is missing for that day.

Figure 7. (a-c) Examples of image quality as defined by visibility at noon. **(a)** clear, **(b)** questionable, **(c)** poor. **(d-f)** Examples of images that would pass noon quality check, but have short term effects on image quality. **(d)** boat passing under Casco Bay Bridge, **(e)** sea bird passing close to camera, **(f)** meteorological phenomena such as sea smoke.

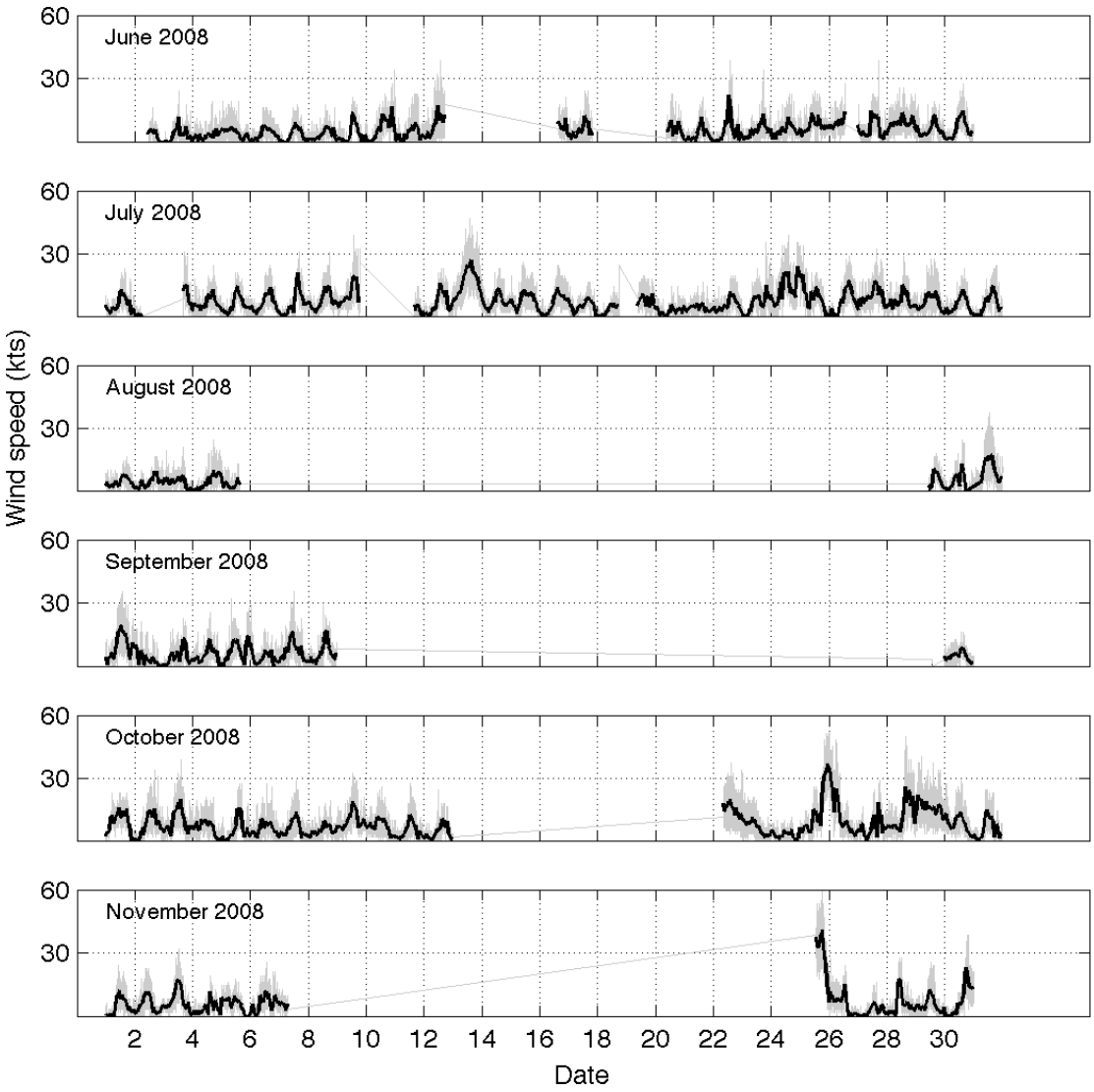

Figure 8. Wind velocity measured at the GMRI meteorological station. Raw data (gray line) and hourly mean (black line).

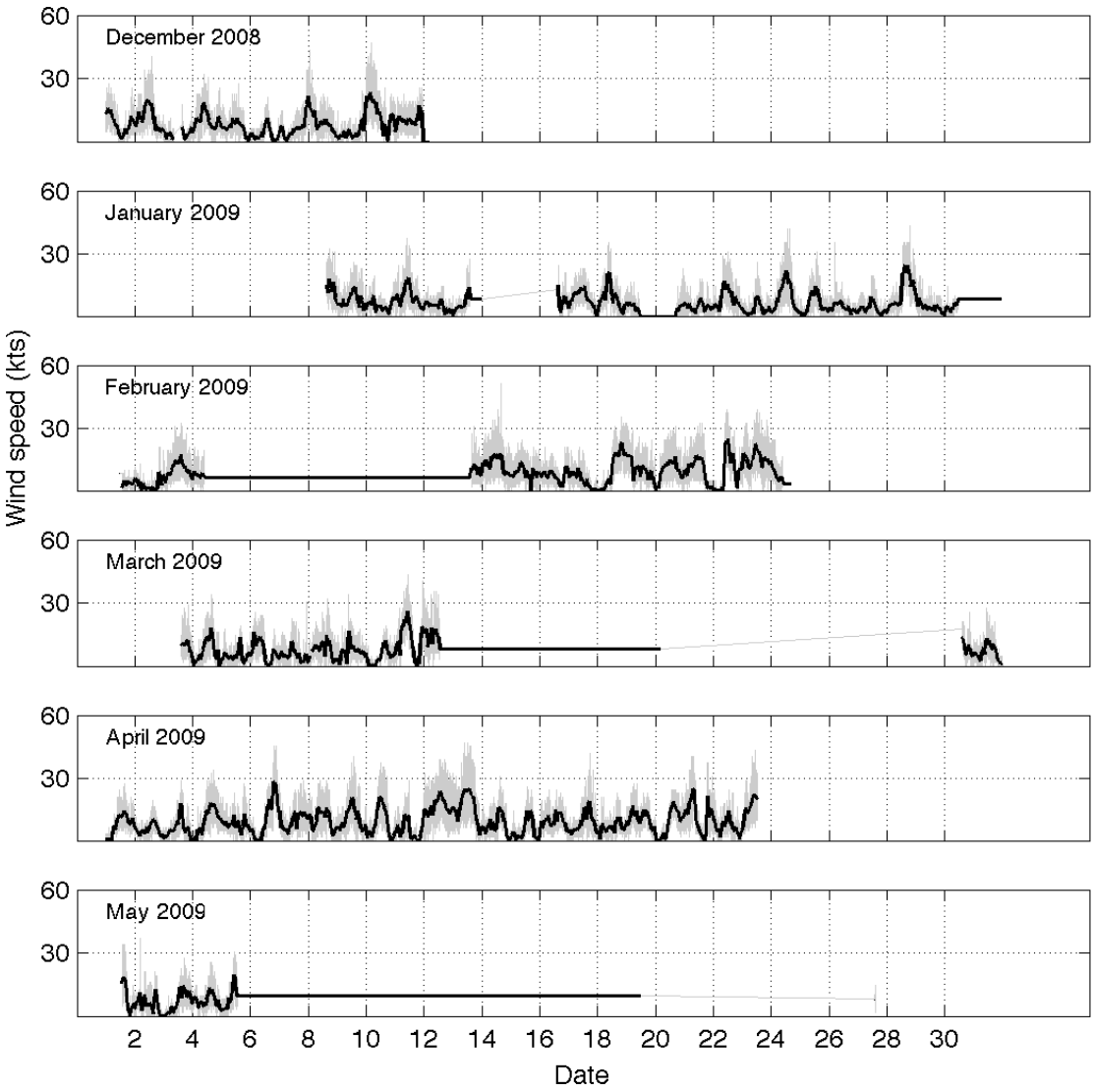

Figure 8 (continued). Wind velocity measured at the GMRI meteorological station. Raw data (gray line) and hourly mean (black line).

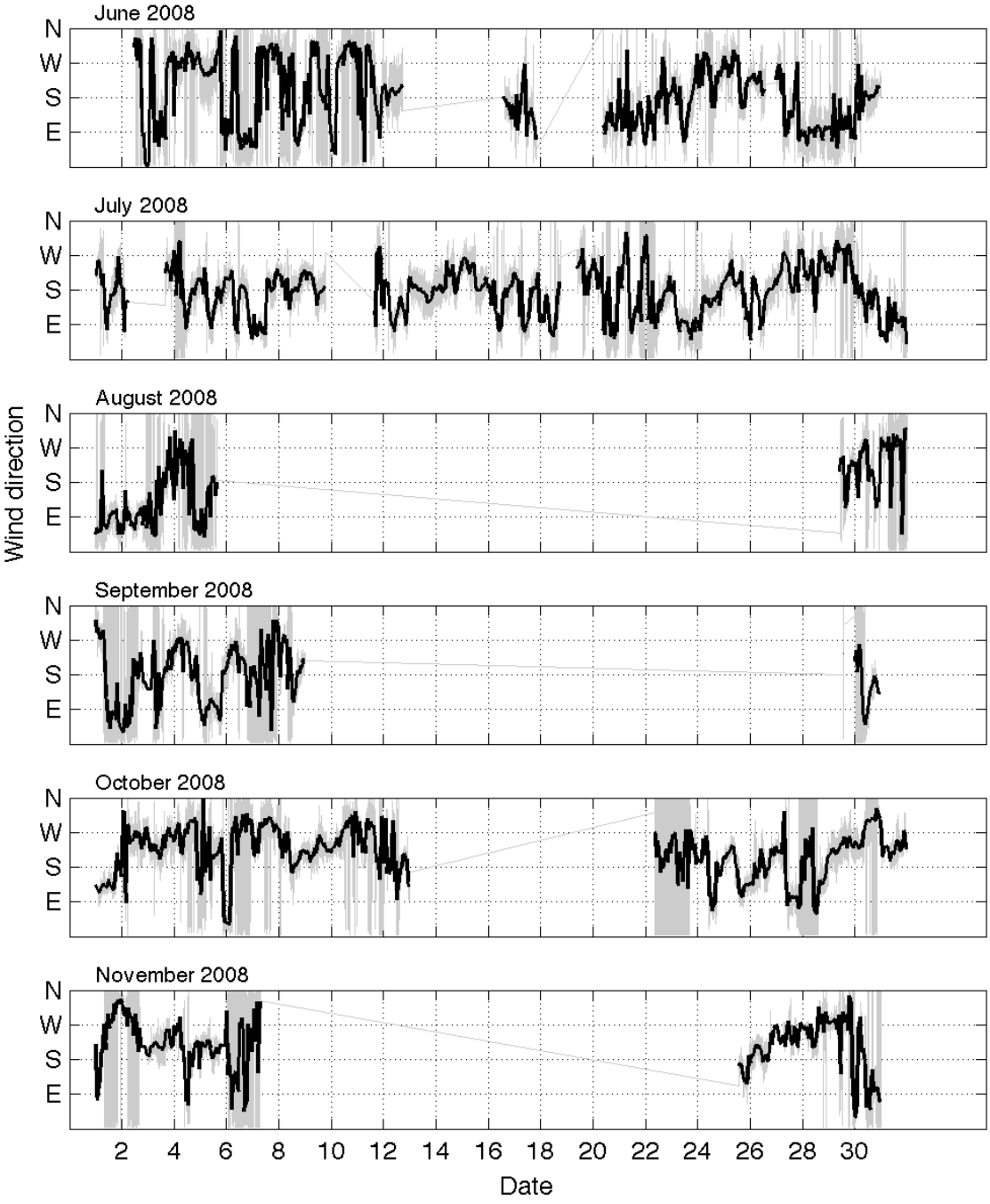

Figure 9. Wind direction measured at the GMRI meteorological station. Raw data (gray line) and hourly mean (black line).

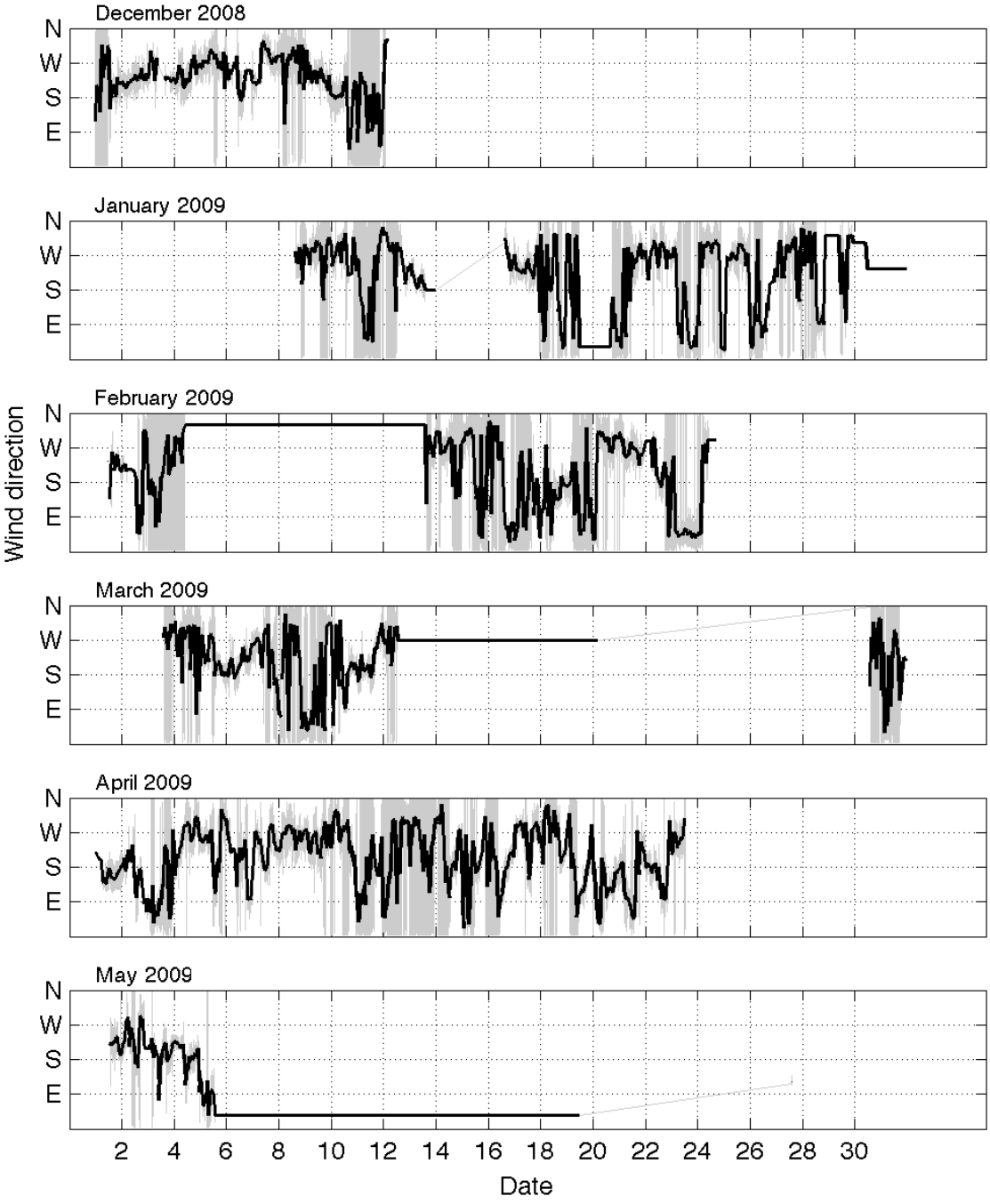

Figure 9 (continued). Wind direction measured at the GMRI meteorological station. Raw data (gray line) and hourly mean (black line).

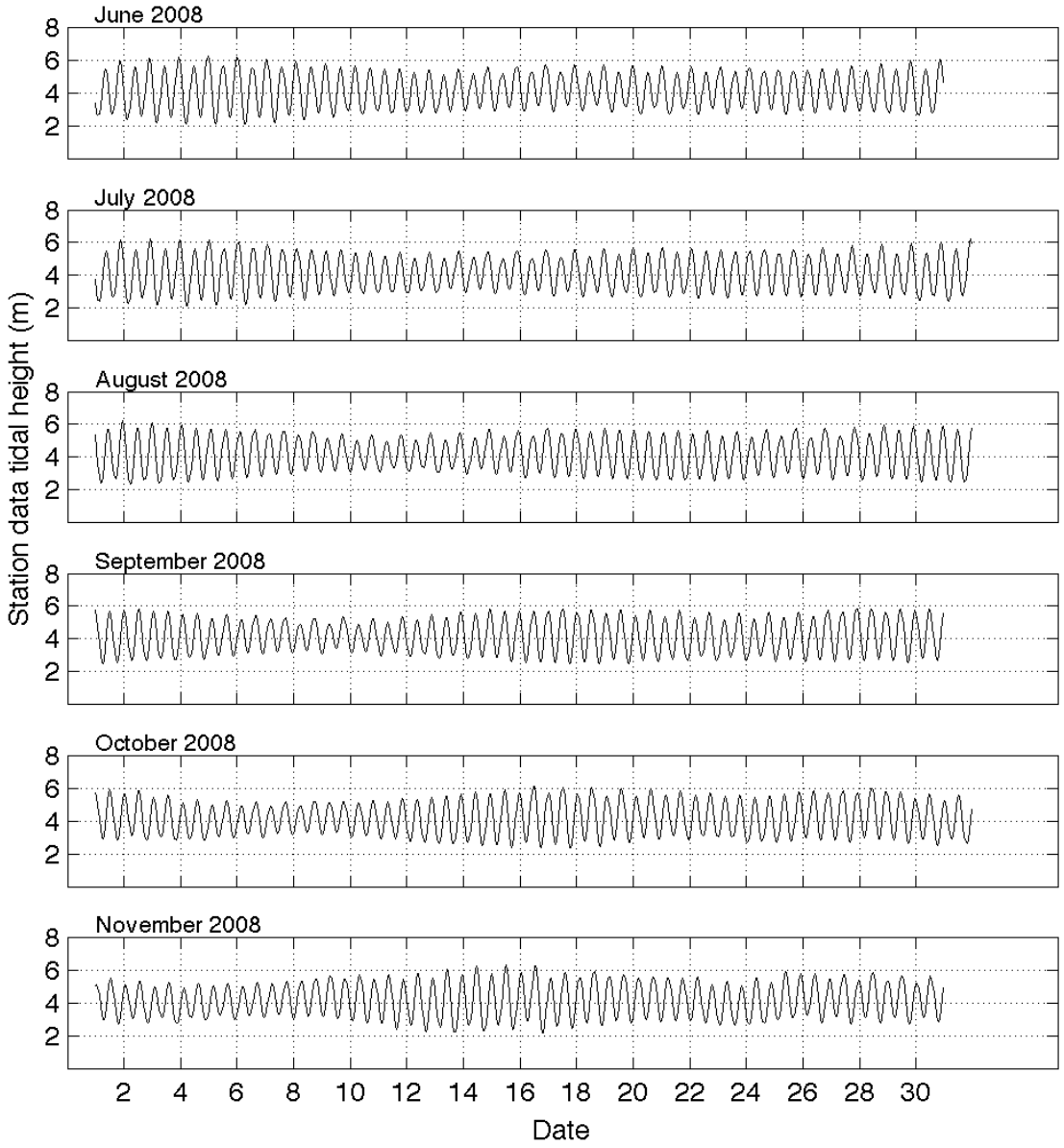

Figure 10. Tidal data from the NOAA tidal gauge (http://tidesandcurrents.noaa.gov/).

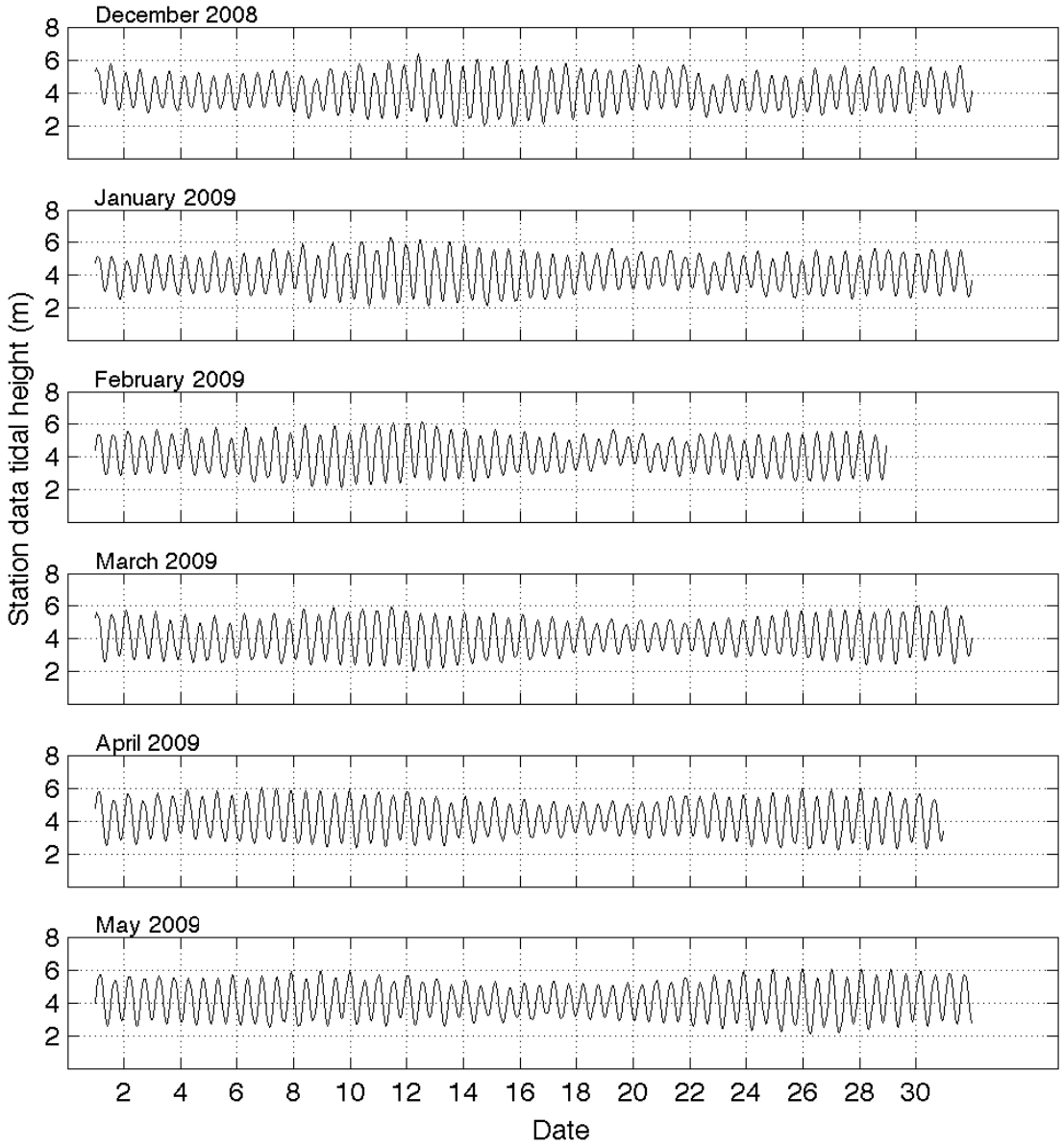

Figure 10 (continued). Tidal data from the NOAA tidal gauge (http://tidesandcurrents.noaa.gov/).

References

Alpers, W. and Espedal, H.A., 2004. Oils and Surfactants. In: Jackson, C.R., Apel, J.R. (Eds.), *Synthetic Aperture Radar Marine Manual,* Natl. Oceanic and Atmos. Admin., Silver Spring, MD, pp 263 – 275.

Bourgault, D., 2008. Shore-based Photogrammetry of St. Lawrence River Ice. Canadian Journal of Civil Engineering, 35, 80 – 86.

Gade, M., Alpers, W., Huehnerfuss, H., Masuko, H., Kobayashi, T., 1998. Imaging of Biogenic and Anthropogenic Ocean Surface Films by the Multifrequency/Multipolarization SIR-C/X-SAR. Journal of Geophysical Research, 103(C9), 18851 – 18866.

Holland K.T., Holman, R.A., Lippmann, T.C., Stanley, J., Plant, J., 1997. Practical Use of Video Imagery in Nearshore Oceanographic Field Studies. IEEE Journal of Oceanic Engineering, 22(1), 81 – 92.

Huehnerfuss, H., Garrett, W.D., Hoge, F.E., 1986. The Discrimination Between Crude-Oil spills and Monomolecular Sea Slicks by an Airborne LIDAR. International Journal of Remote Sensing, 7(1), 137 – 150.

Huehnerfuss, H., 2006. Basic Physiochemical Principles of Monomolecular Sea Slicksand Crude Oil Spills. In: *Marine Surface Films: Chemical Characteristics, Influence on Air-Sea Interactions and Remote Sensing*, Gade, M., Huehnerfuss, H., Korenowski, G. (Eds.), Springer, New York, NY, pp 21 – 35.

Maine Department of Environmental Protection. 1998. *Julie N* Preassessment Data Report. Prepared for Maine Department of Environmental Protection, Maine Department of Conservation, Inland Fish and Wildlife, Department of Marine Fisheries, National Oceanic and Atmospheric Administration, United States Department of the Interior. Industrial Economics, Inc.

Pawlowicz, R., 2003. Quantitative Visualization of Geophysical Flows Using Digital Oblique Time-Lapse Imaging. IEEE Journal of Oceanic Engineering, 28(4), 699 – 710.

Reed, M., Johansen, Ø., Brandvik, P.J., Daling, P., Lewis, A., Fiocco, R., Mackay, D., Prentki, R., 1999. Oil Spill Modeling Towards the Close of the 20th Century: Overview of the State of the Art. Spill Science and Technology Bulletin, 5, 3 – 16.

Thorpe, S. A., 2004. Langmuir Circulation. Annual Review of Fluid Mechanics, 36, 55 – 79.

Wu, J., 1983. Sea-Surface Drift Currents Induced by Wind and Waves. Journal of Physical Oceanography, 13(8), 1441 – 1451.